Machine Learning-Driven Low-Complexity Optical Power Optimization for Point-to-Point Links

Isaia Andrenacci[*,1,2], Matteo Lonardi[2], Petros Ramantanis[2], Élie Awwad[1], Ekhiñe Irurozki[1], Stephan Clémençon[1], Paolo Serena[3], Chiara Lasagni[3] , Sébastien Bigo[2], Patricia Layec[2]

[1]Télécom Paris, 19 Pl. Marguerite Perey, 91120 Palaiseau, France, [2]Nokia Bell Labs, 12 Rue Jean Bart, 91300 Massy, France, [3]University of Parma, Parco area delle Scienze 181/A, 43124, Parma, Italy

**isaia.andrenacci@nokia.com*

Abstract: We propose a strategy to dynamically adjust transmitted power solely based on the analysis of performance fluctuations due to polarization-dependent loss. We show that our method converges faster to optimum compared to a standard approach.

1. Introduction

In today's optical communication networks, in order to accommodate the increasing capacity demand while reducing the cost per transmitted bit, it is necessary to abandon the static set and forget approach that relied on high margins. In response to this challenge, building a real-time, high-fidelity digital replica of the optical network, also known as a digital twin (DT), could allow new designs with enhanced efficiency through margin reduction. Besides, even if a DT is not available [1], a closed loop optimization can be achieved by dynamically adjusting some network parameters and simultaneously verifying by measurements the optimization gains at the receiver end. In this case, machine learning (ML) can play a crucial role in minimizing computational costs.

In this paper, we propose a low-complexity, ML-driven strategy, designed to optimize transmitted optical power, harnessing only signal-to-noise ratio (SNR) fluctuations due to polarization-dependent loss (PDL). This approach builds upon the framework presented in [2], where an ML classifier was used to identify the dominant noise regimes, i.e., linear, dominated by amplifier spontaneous emission (ASE) noise, or nonlinear, dominated by Kerr nonlinearity. Specifically, we leverage, in these regimes, the shape variations of the SNR probability density function (PDF) [3] to quickly attain the optimal power, often referred to as the nonlinear threshold (NLT) [4]. Applying a regression on the transmitted power might be challenging without knowledge of additional network parameters since, within a specific regime, the normalized SNR PDFs exhibit remarkable similarities despite the power differences (e.g., see Fig 4 in [2]). We propose to mitigate the aforementioned challenge by combining two ML classifiers. We demonstrate the potential of our strategy to reach the optimal power regime with a reduced number of iterations compared to an ML-free method relying solely on average SNR, all while maintaining optimal performance levels.

2. Methodology

In Fig. 1 a), we illustrate our closed-loop, ML-driven, input power optimization scheme, for a typical terrestrial link. For simplicity, we assume the system to be homogeneous in terms of fiber types/lengths, while we assume all amplifiers to operate in "constant gain" mode, perfectly compensating for losses. At the transmitter (TX), we employ a fixed grid of 21 channels using Gaussian modulation, while the input power P_{in} [dBm] is adapted to maximize average SNR. The receiver (RX) calculates the standardized moments of the monitored SNR samples (S), i.e., mean, $\mu = \mathrm{E}[S]$, variance, $\sigma^2 = \mathrm{E}[(S-\mu)^2\,]$, skewness, $\gamma = \mathrm{E}[(S-\mu)^3\,]/\sigma^3$, and kurtosis, $\kappa = \mathrm{E}[(S-\mu)^4\,]/\sigma^4$. Then, these moments are used in an input features vector $\boldsymbol{x} = [\mu, \sigma^2, \gamma, \kappa]$ of two ML classifiers, one fine (A) and one coarse (B). We underline the difference with respect to [2] where the entire normalized PDF was used as an input feature vector. Our choice to use moments was made to demonstrate that they sufficiently capture various PDF shapes [3]. Moreover, this definition simplifies ML algorithm's complexity and enhances its interpretability. Each classifier identifies the power range Y_d with $d = \{A, B\}$ where P_{in} is situated. We defined three ranges as follows:1) "LIN_d" with $P_{in} - NLT < \delta_d$, 2) "$NLIN_d$" with $P_{in} - NLT > \delta_d$ and, 3) "MID_d" with $|P_{in} - NLT| \leq \delta_d$. Furthermore, these classifiers provide the prediction probability, defined as $\mathrm{f}_d(\boldsymbol{x}) \triangleq \Pr(\mathrm{Y}_d = y|\mathbf{X} = \boldsymbol{x})$. The classifier A distinguishes itself from B due to its narrower MID range (i.e., $\delta_A < \delta_B$). As it will be discussed next, variable corrections ΔP are applied, according to the classifiers' outputs, i.e., the power ranges Y_d and the associated probabilities $\mathrm{f}_d(\boldsymbol{x})$.

The supervised ML classification algorithms were trained with optical link simulations using the enhanced Gaussian noise (EGN) model extended to account for PDL [3]. The EGN dataset consists of $2 \cdot 10^4$ different PDFs of the SNR for each P_{in} and for each different simulated scenario. Each PDF has been derived from 10^6 SNR samples. Constructing this representative EGN dataset involved exploring various scenarios of TX and link parameters. At TX, the transmitted signals were set to either 49 GBd with 50 GHz spacing or 69 GBd with 75 GHz spacing, while the P_{in} ranged from -10 to $+10$ dBm with a 0.5 dB step size. One reconfigurable add and drop multiplexer (ROADM) was placed after the TX in add mode. The signal was detected after an arbitrary number of spans (12, 15, 18, and 21) of standard single-mode fiber (SSMF) and noisy EDFAs, with all simulation parameters reported in **Error! Reference source not found.** a). The in-line ROADMs featured two wavelength selective switches (WSSs), one in add mode

and the other in drop mode,

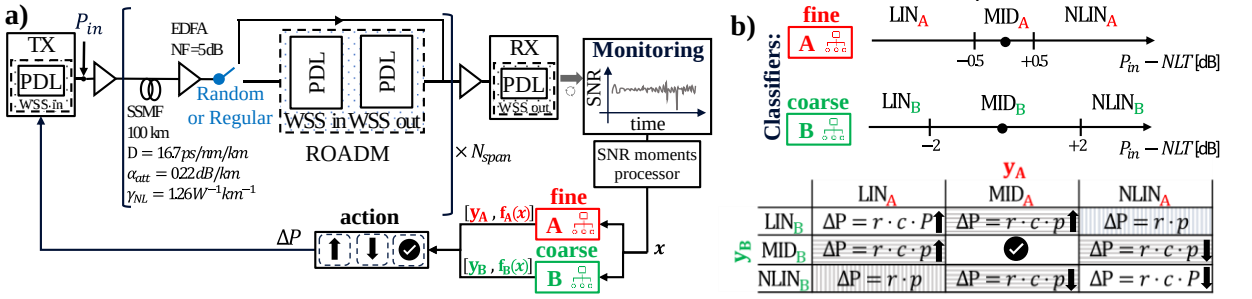

Fig. 1: a) Simulation set up and the ML-driven closed-loop for input power (P_{in}) optimization. Two classifiers $d = \{A, B\}$ are used to define a power correction ΔP from the predicted power ranges (Y_d) and its probability ($f_d(\boldsymbol{x})$). b) Classifiers power ranges and the corresponding power correction, where c, P and p are constant, and $r = \pm 1$.

positioned in two configurations, indicated by the blue switch in Fig. 1 a). The "regular" position of the switch corresponds to a ROADM inserted every three spans, while the "random" position corresponds to a ROADM placed every span with a 30% probability. At the RX, a ROADM is placed in drop mode. To reveal different PDFs shapes, we chose PDL in each WSS with values drawn from two different distributions: a Uniform (U) ranging from 0.1 to 1 dB and a Chi-square (χ^2) with three degrees of freedom, having a mean of 0.21 dB and a probability of exceeding 0.8 dB set at 1.05%. For each scenario, the EGN simulation was repeated with twenty different PDL values.

The collected data was used to create the datasets for the two ML classifiers with each input feature vector $\boldsymbol{x}$ labeled into the corresponding range Y_d. Classifier A is configured with $\delta_A = 0.5$ dB and B with $\delta_B = 2$ dB. This process resulted in two labeled datasets, each containing a total of $2 \cdot 10^4$ instances including all the simulated configurations. For both A and B, we employed the random forest [5] algorithm and we used the macro F1 score [6] as performance metric due to imbalanced Y_d distributions. We divided our datasets into an 80% portion for the training and the 10-fold cross-validation strategy. The remaining 20% of the datasets were used to evaluate the test macro F1 score.

Fig. 1 b) depicts the power adjustment ΔP taken from the ML optimization. The white boxes represent cases where both classifiers agree on the ranges, but this does not guarantee correct classification, as simultaneous errors can occur. If the MID_d range is detected by both classifiers, then $\Delta P = 0$ and optimum power range is assumed for the system. If classifiers agree on either the LIN_d or the $NLIN_d$ range, power adjustments are made by a correction $\Delta P = r \cdot c \cdot P$ where P is set equal to half the MID_B range, i.e., $P = \delta_A = 2$ dB, $c \triangleq 0.5(f_A(\boldsymbol{x}) + f_B(\boldsymbol{x}))$ and $r = \pm 1$. A power reduction ($r = -1$) was considered in the case $NLIN_A$ and $NLIN_B$, otherwise an increase ($r = +1$). The horizontal-filled boxes designate cases where classifiers "slightly disagree", i.e., when adjacent ranges are detected by the classifiers. In this case, a correction of $\Delta P = r \cdot c \cdot p$ is taken, where p is equal to half the MID_B range, i.e., $p = \delta_B = 0.5$ dB. This correction is an input power increment ($r = +1$) if the classifiers predict MID_A (or MID_B) and LIN_B (or LIN_A), while a reduction ($r = -1$) otherwise. In the vertical-filled boxes when classifiers "severely disagree", a correction $\Delta P = r \cdot p$ is chosen when the assigned labels are $NLIN_B$ and LIN_A, if $f_B(\boldsymbol{x}) > f_A(\boldsymbol{x})$, we set $r = -1$, while $r = +1$ when $f_B(\boldsymbol{x}) < f_A(\boldsymbol{x})$. In the case LIN_B and $NLIN_A$ are assigned, a similar rule applies.

To have a fair comparison with ML optimization, we introduced a naïve average SNR-based strategy, relying solely on a set of 10^6 SNR samples. Both approaches start with a $P_{in} = P_0$ that is initially unknown. The naïve strategy adapts power by $(r \cdot \delta P)$ dB with $r = \pm 1$ and $\delta P = 0.5 dB$ in every step, based on the observed average SNR $E[S]$. It starts by randomly choosing r_0 and adjusting the power to $P_{in} = P_0 + r_0 \cdot \delta P$. If $E[S]$ increases, then $r^* = r_0$, otherwise, power is readjusted to P_0 and $r^* = -r_0$.Then the power is iteratively adjusted to $P_{in} + r^* \cdot \delta P$ until a decrease in the average SNR is detected. Finally, it takes one step back and it stops at N^{th} iteration.

3. Results

In Fig. 2 a) we evaluated the cross-validation performance of A and B classifiers using different SNR standardized moments combinations (markers), comparing the results against using the entire normalized PDF (lines), as in [2]. The y-axis represents the macro F1 score, while the x-axis displays the input features combinations. Two key findings stand out from this analysis. Firstly, individual features like skewness (γ) and average SNR (μ) have a significant impact on F1. Skewness is the primary metric for distinguishing between LIN and NLIN ranges as it helps differentiate symmetric PDFs in LIN from asymmetric ones in NLIN. Conversely, μ is essential for identifying the MID-range with the highest SNR. Secondly, both classifiers produce similar scores, suggesting that the choice of the MID-range does not affect the ML performance. Optimal results arise from using all four input features $[\mu, \sigma^2, \gamma, \kappa]$, resulting in an 0.98 test macro F1 score for both classifiers, while only slightly lower scores are achieved by using $[\mu, \sigma^2, \gamma]$ or $[\mu, \gamma]$. Notably, using moments outperforms using the entire PDF, indicating their effectiveness in range identification.

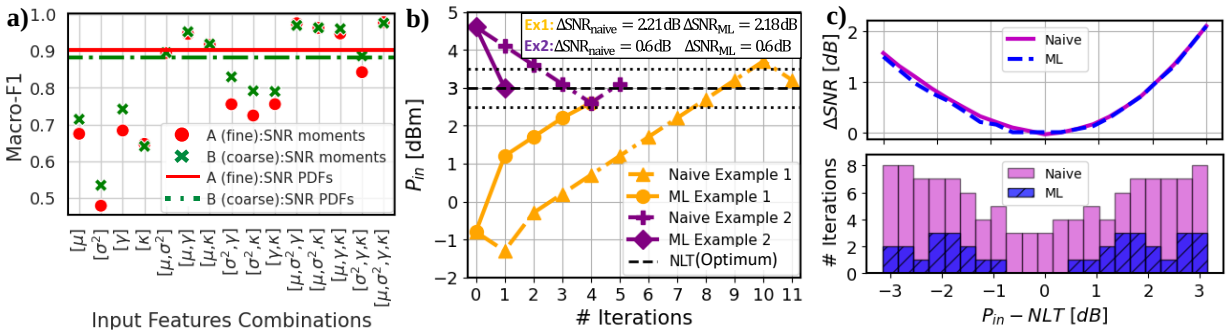

Fig. 2: a) Cross-validation ML performance for Classifiers A (fine) and B (coarse) using the SNR standardized moments combinations (markers) and the normalized PDF (lines). b) ML and naïve optimization convergence speed for two initial power examples: ASE-dominated (Example 1) and Kerr-dominated (Example 2) c) ML and naïve optimization comparison in terms SNR improvement (upper) and required iterations (lower).

Finally, we conducted a comparison between the ML-driven and naïve strategies under a fixed scenario with a symbol rate of 69 GBd, a 75 GHz channel spacing, and random positions of the ROADMs, with their PDL elements set to 0.56 dB. Fig. 2 b) offers a visual representation of the ML and naïve power adjustment, starting from two P_0 values: one in the ASE-dominated regime ($P_0 = -0.8$ dBm, Example1) and one in Kerr-dominated regime ($P_0 = 4.6$ dBm, Example2), for an 18-span link. The y-axis denotes the adjusted P_{in}, while the x-axis represents the number of iterations executed by the optimization strategies. The dotted line represents the desired MID_A range, and the dashed line corresponds to the NLT, in this case equal to 3 dBm. To compare in terms of average SNR improvement, we define $\Delta SNR = \mathrm{E}[SNR_N] - \mathrm{E}[SNR_0]$, where $\mathrm{E}[SNR_0]$ is the average initial SNR corresponding to P_0, and $\mathrm{E}[SNR_N]$ is the one corresponding to P_N. In the Example 2, the ML-driven strategy quickly reaches the optimal range in one iteration, while the naïve approach takes five iterations. In the Example 1, both strategies require more iterations (4 for ML-driven and 10 for naïve), while the naïve approach yields slightly higher SNR improvements. To highlight the trade-off between the number of iterations and SNR improvements in both strategies, we randomly selected various P_0 ranging from -3 dBm to +3 dBm (excluding the training value). Fig. 2 c) presents the optimization results for the two strategies with these selected initial input powers. In the top chart, the y-axis represents the SNR improvements, while the x-axis displays the difference between the P_{in} and the NLT. The bottom histogram uses the same x-axis to represent the number of iterations reported on y-axis. The figure illustrates that we achieved significant SNR improvements in the NLIN range due to the faster SNR decrease compared to the LIN range. The SNR improvements in both strategies are quite similar, with the naïve strategy slightly outperforming the ML strategy in the ASE-dominated range. The ML-based has a significant reduction of the number of iterations, underlining the ML's advantages both near and far from the NLT point. Near NLT, minimal iterations are needed thanks to ML's ability to find the optimal range, while far from NLT, fewer iterations are required due to a bigger power correction.

4. Conclusion

In this study, we introduced an ML technique for input power optimization based on monitored SNR samples in a link with PDL. We utilized two random forest classifiers to categorize SNR standardized moments into three ranges: close to the optimum power, ASE dominant, and Kerr dominant. These classifiers were combined to create a smart optimization of the input power aiming to maximize the average SNR. We compared this approach to a naïve method that relied solely on average SNR with fixed power corrections. Both the ML-driven and naïve techniques resulted in SNR improvements from 0 to 2 dB when the input power was within 3 dB from the optimum. Notably, the ML method required significantly fewer iterations while delivering same or slightly lower SNR improvements with respect to the naïve optimization.

Acknowledgments. *This research was supported by the European Union's B5G-OPEN project with GAN: 101016663*

5. References

[1] A. Gouin et al. "Real-time optical transponder prototype with autonegotiation protocol for software defined networks", JOCN **13**, pp. 224–232 (2021).

[2] M. Lonardi et al. "Kerr Nonlinearity Dominance Diagnostic for Polarization-Dependent Loss Impaired Optical Transmissions". In: 2021 European Conference on Optical Communication (ECOC). Sept. 18, 2021, pp. 1–4.

[3] Paolo Serena, Chiara Lasagni, and Alberto Bononi. "The Enhanced Gaussian Noise Model Extended to Polarization-Dependent Loss", JLT **38**, pp. 5685–5694 (2020).

[4] A. Bononi, N. Rossi, and P. Serena. "On the nonlinear threshold versus distance in long-haul highly-dispersive coherent systems", Opt. Express 20, 204–216, (2012)

[5] Leo Breiman. "Random forests". In: Mach. learning 45 (2001), pp. 5–32.

[|6] D. Powers. "Evaluation: From Precision, Recall and F-Factor to ROC, Informedness, Markedness & Correlation", Mach Learn. Technol. **2**, (2008).